Plant Physiology Preview. Published on May 22, 2009, as DOI:10.1104/pp.109.139139

Running Head: Novel P- and N-responsive microRNAs

Corresponding author:

Wolf-Rüdiger Scheible
Max-Planck Institute of Molecular Plant Physiology
Science Park Golm
Am Mühlenberg 1
14476 Potsdam, Germany

Tel.: +49 331 5678155
E-mail: scheible@mpimp-golm.mpg.de

Research Category: Environmental Stress and Adaptation

Identification of nutrient-responsive *Arabidopsis* and rapeseed microRNAs by comprehensive real-time PCR profiling and small RNA sequencing[*]

Bikram Datt Pant[†], Magdalena Musialak-Lange[†], Przemyslaw Nuc[†], Patrick May[†], Dirk Walther, Wolf-Rüdiger Scheible[§]

Max-Planck Institute of Molecular Plant Physiology, Science Park Golm, Am Mühlenberg 1, 14476 Potsdam, Germany.

Footnotes:

* The work was supported by the Max-Planck Society.

† These authors contributed equally to the results.

§ Corresponding author (e-mail: scheible@mpimp-golm.mpg.de).

ABSTRACT

Comprehensive expression profiles of Arabidopsis (*Arabidopsis thaliana*) *MIRNA* genes and mature microRNAs (miRs) are currently not available. We established a quantitative real-time PCR (qRT-PCR) platform that allows rapid and sensitive quantification of 177 Arabidopsis primary miR transcripts (pri-miRs). The platform was used to detect phosphorus (P) or nitrogen (N) status-responsive pri-miR species. Several 169 family pri-miRs as well as pri-miR398a were found to be repressed during N-limitation, whereas during P-limitation pri-miR778, 827 and 399s were induced and pri-miR398a was repressed. The corresponding responses of the biologically active, mature miRs were confirmed using specific stem-loop RT primer qPCR assays and small RNA sequencing. Interestingly, the latter approach also revealed high abundance of some miR star strands (miR*). Bioinformatic analysis of small RNA sequences with a modified miRDeep algorithm led to the identification of the novel P-limitation induced miR144, which is encoded by two loci in the Arabidopsis genome. Furthermore, miR144, miR169, a miR827-like sequence and the abundances of several miR*s were found to be strongly dependent on P- or N-status in rapeseed (*Brassica napus*) phloem sap, flagging them as candidate systemic signals. Taken together, the results reveal the existence of complex small RNA-based regulatory networks mediating plant adaptation to mineral nutrient availability.

INTRODUCTION

During recent years ~21 nucleotide long microRNAs (miRs) have been recognized as important regulators of gene expression in animals and plants (Bartel, 2004; Dugas and Bartel, 2004; Kidner and Martienssen, 2005; Chuck *et al.*, 2009). In plants, miRs were shown to post-transcriptionally regulate diverse aspects of development like leaf polarity (Emery *et al.*, 2003), leaf shape (Palatnik *et al.*, 2003), the transition from the juvenile to the mature growth phase (Wu and Poethig, 2006), flowering time (Aukerman and Sakai, 2003), stomatal development (Kutter *et al.*, 2007) or nodule development (Combier *et al.*, 2006).

MiRs also regulate the adaptation of plants to abiotic stresses including macronutrient limitations (Sunkar and Zhu, 2004; Fujii *et al.*, 2005; Bari *et al*, 2006; Chiou *et al.*, 2006; Sunkar *et al.*, 2007). MiR395 and miR399 have been shown to be specifically induced during sulfur- and phosphorus-limitation, respectively (Jones-Rhoades and Bartel, 2004; Fujii *et al.*, 2005; Bari *et al.*, 2006; Chiou *et al.*, 2006; Kawashima *et al.*, 2008). MiR399 targets the transcript of an E2-conjugase that is mutated in phosphate (Pi)-accumulating *Arabidopsis pho2* mutants, and this phenotype is recapitulated in miR399 over-expressing plants (Aung *et al.*, 2006; Bari *et al.*, 2006). MiR399 presumably acts in a dualistic manner to inhibit PHO2. It promotes transcript decay (Allen *et al.*, 2005; Bari *et al.*, 2006) but also appears to inhibit *PHO2* expression by repressing translation (Bari *et al.*, 2006), a mechanism that is probably widespread in plants (Aukerman and Sakai, 2003; Brodersen *et al.*, 2008). Recently, miR167 has been associated with lateral root outgrowth in response to nitrogen-limitation (Gifford *et al.*, 2008). Pri-miR167a was shown to be ~5-fold repressed by nitrogen in root pericycle cells, permitting the target *ARF8* transcript to accumulate and initiate lateral root outgrowth. Furthermore, miR398 was reported to be down-regulated by oxidative stresses and copper limitation, but induced by sucrose, and thereby repressing two Cu/Zn superoxide dismutases and a cytochrome c oxidase subunit (Sunkar *et al.*, 2006; Yamasaki *et al.*, 2007; Dugas and Bartel, 2008).

Despite these examples, little information about stress- or nutrient-responsive plant miRs is available. This is due to their often low expression levels and the absence of miR or *MIRNA* gene probes on widely-used transcriptomics platforms such as Affymetrix GeneChips®. Custom-made microarrays can be designed to include probes for miRs and *MIRNA* genes for a broader response analysis, but these are not very sensitive (e.g. Axtell and Bartel, 2005; Liu *et al.*, 2008). Reverse transcription followed by quantitative polymerase chain reaction analysis (qRT-PCR) with non-specific double-stranded DNA binding

fluorophores, such as SYBR green, is a powerful alternative for highly sensitive, rapid, multiparallel and cost-effective expression analysis (Udvardi *et al.*, 2008). Shi and Chiang (2005) and Chen *et al.* (2005) reported two qRT-PCR-based methods to measure the levels of mature miRs. The first approach relies on *in vitro* polyadenylation of mature miRs followed by reverse transcription with an oligo-(dT) adapter primer and amplification using SYBR green, with a miR-specific forward primer and a compatible reverse primer. In the second approach, each specific miR is reverse-transcribed from total RNA using a specific stem-loop primer, followed by TaqMan PCR amplification. Although it is desirable to quantify the biologically active mature miR species, a limitation of both qRT-PCR methods is that they are unable to differentiate the expression strengths of *MIRNA* genes that yield (near-) identical mature miR molecules. Hence, the interpretation of the results will be dominated by strongly expressed member(s) of a given *MIRNA* gene family, while the contribution of lowly expressed members will go unnoticed. This might be especially important if these genes are expressed in an organ- or cell type-specific manner.

Deep-sequencing using new technologies, e.g. Illumina-Solexa chemistry, is another approach being adopted for the analysis of small RNA / miR abundance (German *et al.*, 2008; Moxon *et al.*, 2008a; Szittya *et al.*, 2008). The high number of sequence reads promises sensitivity, yet the necessary expertise required and the labor and cost involved are considerable. Data from small-RNA sequencing together with miR prediction algorithms like miRDeep (Friedländer *et al.*, 2008) also provide the basis for discovery of novel miRs, even in organisms that have been specifically surveyed to identify miRs.

We have developed a qRT-PCR platform for parallel analysis of 177 currently known Arabidopsis *MIRNA* gene primary transcripts (pri-miRs). This platform provides a sensitive, yet inexpensive tool for Arabidopsis researchers to carry out miR expression analysis. A comparable approach has previously been described for monitoring expression of 23 human miR precursors (Schmittgen *et al.*, 2004). As pri-miRs are generated by RNA polymerase II in plants and animals (Bracht *et al.*, 2004; Cai *et al.*, 2004; Kurihara and Watanabe, 2004; Lee *et al.*, 2004) they contain 5' caps and 3' poly(A) tails. The latter make the transcripts amenable to oligo-(dT)-primed reverse transcription and thus multi-parallel analysis by qRT-PCR. Although pri-miRs are not the biologically active molecules, several previous studies have shown that the response of a pri-miR can reflect the one of the encoded mature miR (Jones-Rhoades and Bartel, 2004; Bari *et al.*, 2006; Pant *et al.*, 2008) and thus can serve as a valid indicator. QRT-PCR profiling of pri-miRs can therefore serve as a useful tool to discover

responses to particular stimuli, which can then be confirmed by analysis of the mature species.

In this work we first established the pri-miR platform and then used it to discover previously unknown nutrient-responsive pri-miRs. The corresponding mature miRs were investigated by targeted assays and further confirmed by small-RNA sequencing, which also revealed novel insights. The results indicate that small RNAs play a much more important role in nutrient-signaling than previously thought.

RESULTS

A qRT-PCR platform for Arabidopsis pri-miRs.

Sequences of 184 annotated Arabidopsis miR stem-loops were obtained from the miRBase database (www.microrna.sanger.ac.uk). These sequences are not strictly precursor miRs (pre-miRs), but may include flanking sequence from the presumed pri-miR. Pri-miR sequences of members from the same family can be almost identical, complicating the design of specific PCR primers. This occurs in the miR169 family, where mir169i through miR169n are located in three highly homologous, tandem-arrayed stretches (Supplemental Figure 1), and in the miR854 family, where the pre-miR sequences of the four annotated members are 97 to 100% identical. However, it is questionable whether miR854s are true miRs, as. the sequences are located close to (or in) the centromere of chromosome 5 and are annotated as transposable elements in the TAIR database (www.arabidopsis.org). Therefore we treated miR854 as a single miR, leaving a total of 181 sequences for which primers were designed.

To ensure maximum specificity and efficiency during PCR amplification of pri-miR cDNA under a standard set of reaction conditions (cf. Figure 1A), a stringent set of criteria was used for primer design (cf. Materials and Methods). PCR primers were tested on cDNA from Arabidopsis wild-type Col-0 seedlings, which was free of genomic DNA contamination. Using this cDNA as template, 150 primer pairs gave unique PCR products of the expected size, while 27 primer pairs yielded no product and four gave unspecific products. The 27 primer pairs were retested using Arabidopsis Col-0 genomic DNA as template. 15 primer pairs resulted in the expected genomic product, showing that the primers anneal to the correct sequence, and suggesting that the targeted pri-miRs (e.g. 159c, 166c, 395a-f or 404, cf. Supplemental File 2) were either below the detection limit in the cDNA samples or that amplification from the cDNA was inhibited. Evidence in support of the former hypothesis comes from the observation that some of the primers, e.g. pri-miR395a-f, did amplify the

expected products from a cDNA sample derived from sulfur-limited seedlings (Supplemental Figure 2). The 16 primer pairs that did yield any product from cDNA or genomic DNA templates, or amplified unexpected/unspecific products were redesigned, finally resulting in 175 validated primer pairs and only six *MIRNA* genes (highlighted in red in Supplemental File 2) for which no working pairs could be established.

Specificity of PCR primers was assessed by melting curve analysis of PCR reaction products (Supplemental Figure 3), by separating the PCR products via electrophoresis in high-resolution agarose gels (Figure 1B), and by double-stranded sequencing of a subset of the pri-miR PCR products (Supplemental Figure 4). In all cases the sequences of the PCR products were identical to those of the intended pri-miR targets. The average amplification efficiency (E) of the primers, as determined by LinRegPCR (Ramakers *et al.*, 2003), was high; for 102 primer pairs E was >90% and for another 39 pairs E was 81-90% (Figure 1C, Supplemental File 2). 21 primer pairs did amplify a correct product from genomic DNA, but no product was obtained with cDNA from the samples investigated (see below); hence no E value could be established for these primers.

The fraction of pri-miRs detected, i.e. expressed in at least two biological replicates with a threshold fluorescence cycle number C_T <40 was just below 80%, irrespective of the growth conditions tested (cf. Supplemental File 2). This percentage is comparable to the percentage of transcription factor (TF) genes detected at this threshold (~83%; Czechowski *et al.*, 2004). However, the average ΔC_T value of pri-miRs was higher than for the TF gene transcripts (Figure 1D). Hence, pri-miRs are often less abundant than TF transcripts. Low abundance (C_T > 33) also resulted in higher variability between replicate measurements, making detection of small expression changes less reliable.

Identification of N- and P-responsive Arabidopsis pri-miRs.

The qRT-PCR platform was used to identify pri-miRs that are induced or repressed in 9-day-old Arabidopsis seedlings during nitrogen (N) or phosphorus (P) limitation (Supplemental File 2). The expected physiological status of the seedlings was confirmed by evaluation of marker gene expression (Supplemental Figure 5). *NRT2.5* (*At1g12940*) and *AMT1.5* (*At3g24290*) were both strongly induced in N-limited seedlings, and *PHT1.4* (*At2g38940*) was induced by P-limitation as found previously (Scheible *et al.*, 2004; Morcuende *et al.*, 2007).

Twenty pri-miRs exhibited differential expression in N- or P-limited conditions (Figure 2), based on an average change in normalized cycle number of at least three ($|\Delta\Delta C_T|$

≥ 3) between nutrient limitation and full nutrition (FN). The most prominent change was the known induction of pri-miR399s during P-limitation, with $\Delta\Delta C_T$ ranging from 6.5 to 20 (Figure 2, cf. Bari *et al.*, 2006). Pri-miR399d was undetectable in FN conditions and rose to levels comparable to some of the most strongly expressed genes in Arabidopsis, such as *UBQ10* (cf. Czechowski *et al.*, 2005). Very high expression of pri-miR399s and mature miR399 during P-limitation is necessary to fully suppress the activity of its target *PHO2* transcript (Bari *et al.*, 2006). Mechanistically this seems to involve translational repression as suggested by previous results (Bari *et al.*, 2006) and our finding that miR399d over-expressing seedlings have levels of substantially lower but still detectable levels of *PHO2* transcript (10-20% of control plants), while their molecular phenotypes are identical to *pho2* seedlings (Supplemental Figure 6).

QRT-PCR profiling revealed several pri-miR species for which nutrient-responsiveness was previously unknown: pri-miR447c, 778, and 827 all increased ($\Delta\Delta C_T$ = 4.2 – 7.6) during P-starvation, whereas pri-miR398a strongly decreased ($\Delta\Delta C_T$ = -6.9) (Figure 2; Supplemental File 2). Also pri-miRs 169m and 169n displayed induction ($\Delta\Delta C_T$ = 3.7 – 4.2) during P-limitation, and the same two pri-miR169s plus five additional ones (pri-miR169h through 169l) were decreased ($\Delta\Delta C_T$ = -3.1 – -4.9) in N-limited seedlings (Figure 2).

Pri-miR398a and pri-miR447c were not only responsive to P-limitation but also showed a similar response in N-limitation albeit not as strong; with pri-miR398a being slightly repressed ($\Delta\Delta C_T$ = -2.45; cf. Supplemental File 2) and pri-miR447c induced ($\Delta\Delta C_T$ = 3.5) (Figure 2). Furthermore, pri-miRs156e, 156g and 157d were found to be induced ($\Delta\Delta C_T$ = 3.1 – 4.4) in N-limited seedlings. Pri-miR167a, which was reported to be more highly expressed in N-limited root pericycle cells (Gifford *et al.*, 2008) showed no clear response in our experiments with N-limited seedlings. However, pri-miR167d was less expressed ($\Delta\Delta C_T$ = -2.5) in N-limited seedlings (cf. Supplemental File 2).

Nutrient-responsive mature miR species.

To examine if the mature miRs derived from the nutrient-responsive pri-miRs also showed a nutrient response, we used a qRT-PCR approach similar to the one described by Chen *et al.* (2005) (cf. Supplemental Table 1). In addition to nutrient-replete (FN), N-limited (-N) and P-limited (-P) Arabidopsis seedlings, we also included carbohydrate-limited (-C) seedlings (cf. Supplemental Figure 5) in the analysis. Mature miR399s were not analyzed, since their high abundance during P-limitation is already well documented (see introduction).

MiR778 and miR827 were both strongly induced by P-limitation, thus confirming the response of their pri-miRs. However, they did not respond to either N- or C-limitation (Figure 3), and remained almost undetectable under these conditions, suggesting that both of these miRs are involved in P-specific regulation events. The response of miR398a was also similar to that of the corresponding pri-miR, being decreased by P- and N-limitation, and also by C-limitation (Figure 3).

Given the previous report of Gifford *et al.* (2008) and the moderate repression of pri-miR167d we observed in N-limited seedlings, we also investigated miR167. The assay for miR167 showed a relatively high expression level ($40-\Delta C_T = 35$), but this might be due to low specificity in the assay leading to detection of miR167 derived from several primary transcripts. Our result obtained with N-limited seedlings (Figure 3) does not confirm the reported down-regulation of miR167 in root pericycle cells by organic nitrogen (Gifford *et al.*, 2008). Possible explanations for this discrepancy are the non-specificity of the assay for miR167 and/or the lack of spatial resolution in our analysis, which could mask any cell-type specific response of a particular *MIRNA* gene and its derived miR.

Nucleolytic cleavage of pri-miR169h-n (cf. Supplemental Figure 1) by the DICER endoribonuclease results in identical miR169 molecules, precluding a specific assay. Nonetheless, since all seven pri-miR sequences were less abundant in N-limitation (Figure 2), we were able to confirm lower miR169h-n levels in N-limitation (Figure 3). The moderate induction found for two of these pri-miR169 species during P-limitation was not supported by the miR169h-n assay; on the contrary, mature miR169h-n showed a significant (~3-fold) decrease in P-limitation. A second assay designed for miR169a-g also indicated lower abundance during N- and P-limitation (Figure 3), although no clear change was detected for the corresponding pri-miRs.

We were also able to confirm a slight induction ($\Delta\Delta C_T \sim 2$) of miR447 during P- but not N-limitation, whereas the induction of miR156 during N-limitation, as suggested by pri-miR156e and 156g (Figure 2) was not confirmed (Figure 3). Again, a non-specific assay and high expression of other pri-miRs from the same family (Supplemental File 2) probably account for this discrepancy.

P-status responsive miRs detected by small RNA sequencing.

As an independent approach to verify the P-responsiveness of mature miRs we used small RNA sequencing (SRS) with Illumina Solexa technology. Three cDNA libraries prepared from nutrient-replete (FN) seedlings, P-limited (-P) seedlings, and -P seedlings that were

resupplied with 3mM phosphate for three hours (3hP) were sequenced (cf. Supplemental Table 2). Sequence reads with 100% identity to Arabidopsis pre-miRs were extracted, identical reads totaled (Supplemental Table 2, Supplemental Figure 7, Supplemental File 3) and normalized for each library. A plot of the distribution of read lengths for pre-miR-matching sequences (Supplemental Figure 7A) illustrates that these consist almost exclusively of 20- and 21-mers, with the latter being the most abundant, whereas a plot of all genome matching sequences reveals a substantial number of 24-mers and other lengths (Supplemental Figure 7B). Comparison also shows a significantly (~30%) higher number of 21-mers in the group of genome-matching sequences, possibly indicating the presence of unknown miRs.

The normalized read numbers for miR399s were high during P-limitation and very low in nutrient-replete (FN) conditions (Figure 4A), as expected (cf. Bari *et al.*, 2006; Pant *et al.*, 2008). There was no appreciable decrease of miR399s three hours after Pi re-addition, supporting earlier results which suggested that miR399s are rather stable (Bari *et al.*, 2006). SRS also confirmed high expression of miR778 and miR827 during P-limitation (Figure 4A). Very few (1 or 2) or no reads were obtained for miR398a, 447c, 845 or 169h-n, whereas these miRs were detectable by qRT-PCR, suggesting that our qRT-PCR analysis was more sensitive than the SRS approach. SRS showed three additional miRs, i.e. miR408, miR829 and miR863, to be 4 to 10-fold more abundant during P-limitation. Analysis by qRT-PCR supported the increase in levels of miR408, but was unable to confirm the higher abundance of miR829 or miR863 (Supplemental Figure 8).

Surprisingly, sequence reads representing star (*) strands of some of the nutrient-responsive miRs (i.e. miR398a*, miR399a*, miR399c*, miR399d*, miR399f* and miR778*) were found to be present in numbers similar to, or exceeding (up to 200-fold in the case of miR398a*) those for the corresponding miRs (Figure 4A, Supplemental File 3), whereas others (e.g. miR399b*, miR827* or miR863*) were absent. The presence of star strands and their specific induction by Pi-limitation was confirmed by qRT-PCR (Supplemental Figure 8). These results raise the question of the biological function of these abundant miR*s. Another interesting observation from the SRS was that the sequence reads corresponding to miR778 and miR863 do not perfectly agree with the annotated miR sequences determined from flower samples (Fahlgren *et al.*, 2007), but look to be shifted by one or several nucleotides (Supplemental File 3). Furthermore, the miR778/miR778* duplex appears to be unusual in having a 5'-overhang, which is 7-nt long (Supplemental File 3). These results from Arabidopsis seedlings could indicate that the cleavage site of some pre-miRs by DICER proteins is not totally fixed, and may change with developmental age.

Discovery of a novel P-status responsive miR.

The SRS data were analyzed further to look for novel P-status dependent miRs. Candidate miRs were predicted using a miRDeep algorithm (Friedländer *et al.*, 2008) that was adapted for plant miR precursor sequences (P. May, M. Friedländer, unpublished). Among the predicted miR candidates was one, named miR144, which showed a very strong dependence on P-status (Figure 4A). It is highly abundant during P-limitation but almost absent in nutrient-replete seedlings, and so closely resembles the behavior of known P-responsive miRs - miR399s, miR778, and miR827-, in these conditions. When Pi is resupplied to Pi-limited seedlings, the abundance of the novel miR144 fell by ~2-fold within three hours of Pi re-addition (Figure 4A). This response differs from miR399s and miR827, which do not fall rapidly after Pi re-addition, but is similar to miR778, suggesting that the biological half-life times of miRs can vary considerably.

The DNA sequence of miR144 is present twice in the Arabidopsis genome; upstream of *At5g02040*, and between *At3g09280* and *At3g09290*. For these locations, the algorithms mirDeep and mirCat (http://srna-tools.cmp.uea.ac.uk) predicted two precursor sequences / structures, named pre-miR144a and b (Figure 4B). The observation that the read numbers of the two star strands (miR144a*, miR144b*) are similar and that they decrease after Pi re-addition or are almost absent in P-replete conditions, reveals that both loci have P-responsive expression and contribute to a similar extent. The strong P-limitation response of miR144 was confirmed by qRT-PCR (Supplemental Figure 8). In addition, PCR products designed to encompass larger stretches (82 and 103 nt) of pre-miR144a and b could be amplified from oligo-(dT)-primed cDNA pools, showing that miR144 is derived from polyA-tailed primary transcripts, and these also displayed strong P-responsiveness (Figure 4C). Furthermore, both the mature miR144 and its pri-miRs displayed specificity for P, as N- or C-limitation did not affect the expression levels (cf. Figure 4C, Supplemental Figure 8). We were also able to find potential orthologs of pre-miR144s in rapeseed (*Brassica napus*) (Supplemental Figure 9). The rapeseed 144a and 144b precursors share 83 and 85% identity at the DNA level with their Arabidopsis counterparts and are predicted to fold into stable extended hairpin structures by the miRCat algorithm. PCR primer pairs for Arabidopsis pri-miR144a and 144b were added to the qRT-PCR platform, thus bringing the number of *MIRNA* genes represented to 177 (Supplemental File 2).

MiRs with P- or N-status dependent abundance in rapeseed phloem sap.

MiR399 was previously found to be highly abundant in phloem sap from rapeseed and pumpkin during P-limitation, and to constitute a shoot-derived long-distance signal for the regulation of plant phosphate homeostasis (Buhtz *et al*., 2008; Lin *et al.*, 2008; Pant *et al*., 2008). To test whether additional miRs show nutrient-status dependent abundance in phloem sap, we collected sap from nutrient-replete, P-limited and N-limited rapeseed plants and prepared small RNA libraries for sequencing.

Analysis of the resulting small RNA reads (cf. supplemental Table 3) showed that sequences homologous to miRs known to be present in the phloem (e.g. miR156, miR159, miR167) were present in the libraries, whereas sequences homologous to miR171, which is abundant in leaf or stem tissue but undetectable in phloem (Yoo *et al.*, 2004; Buhtz *et al.*, 2008), were completely absent (Figure 5A). This indicates that the phloem sap samples were not noticeably contaminated with small RNAs from stem tissue. Small RNA species found in the libraries should thus represent authentic phloem constituents. The high purity of rapeseed phloem sap obtained using the same method was previously reported by Giavalisco *et al*. (2006) and Buhtz *et al*. (2008).

Further analysis revealed that in addition to *Bna*-miR399 (Figure 5B, Pant *et al.*, 2008), a *Bna*-miR399-like sequence, *Bna*-miR144, a *Bna*-miR144-like sequence and an *Ath*-miR827-like sequence are highly abundant in rapeseed phloem sap during P-limitation, while no sequences homologous to the P-responsive *Ath*-miR778 were found. We were also able to determine that: (i) two sequences with homology to *Ath*-miR399d* and *Ath*-miR399f*, (ii) *Bna*-miR144a* and *Bna*-miR144b* and (iii) five miR144*-like sequences were clearly present in phloem sap during P-limitation, but absent or much less abundant in phloem sap of nutrient-replete or N-limited rapeseed (Figure 5B). Furthermore, we found *Bna*-miR169m to be present in phloem sap of nutrient-replete plants, and the relative abundance of this species strongly decreased in phloem sap of N-limited or P-limited rapeseed plants (Figure 5B). These results pinpoint miR144s, miR144*s, miR399*s, miR827 and miR169 as novel candidate long-distance signals for reporting P- or N-status in the plant system, and suggest an expansion of the miR144 family in rapeseed.

Target predictions for nutrient-regulated miRs.

To identify candidate miR target genes we used four prediction algorithms: miRU (Zhang, 2005), target search in WMD2 (Ossowski *et al.*, 2008), the prediction tool in the UEA plant sRNA toolkit (Moxon *et al.*, 2008b) and PITA (Kertesz *et al*., 2007). In addition, we mined experimental data from degradome studies (Addo-Quaye *et al*., 2008; German *et al.*, 2008).

The first three algorithms score the complementarity of miR and target RNA sequences based on established rules, e.g. the 'seed rule' (Allen *et al.*, 2005), thereby also exploring the observation that plant miRs seem to bind almost perfectly to their cognate mRNAs (Rhoades *et al.*, 2002; Lai, 2004). In contrast, PITA assesses site accessibility in miR target recognition. This includes prediction of target RNA secondary structure and calculation of the free energy gained from the formation of the miR-target duplex and the energetic cost of unpairing the target to make it accessible to the miR. All candidate miR targets predicted with miRU, WMD2 or the UEA plant sRNA toolkit, and up to 20 best targets from the PITA analysis are shown in Supplemental File 4, with a selection of the predicted targets shown in Table I.

In addition to the confirmed miR399 target *PHO2*, a potential target of miR399b/c predicted by all algorithms is the receptor kinase gene *ACR4*, which restricts formative cell divisions in the Arabidopsis root (De Smet *et al.*, 2008). Another repeatedly predicted miR399b/c target is *At4g00170* encoding a vesicle-associated membrane protein. A DEAD-box helicase gene (*At4g09730*) appears as a candidate miR399a/d target from analysis with conventional prediction algorithms, whereas PITA analysis identifies *IPS1*, a miR399 target-like interactor (Franco-Zorilla *et al.*, 2007). There are also clear target predictions for miR399*s with *At3g11130*, encoding a clathrin heavy chain and thus another protein involved in vesicle transport in the secretory pathway, being a potential target of miR399d*. One of the best potential targets of miR399f* is the *CLAVATA3*-related *At3g25905*/*CLE27*, a gene encoding a small peptide that is highly expressed in shoot apices (Sharma *et al.*, 2003).

Obvious targets of miR827 are the E3 ligase gene *NLA* (*At1g02860*) and its homolog *At1g63010* (Table I, Fahlgren *et al.*, 2007). Also miR144 is predicted to target an E3 ligase gene (*At3g27150*) and a calcineurin-like phosphoesterase gene (*At1g07010*). A likely target of miR778 is the histone methyltransferase gene *SUVH6* (*At2g22740*), with *SUVH5* (*At2g35160*) being a possible target as well. Interestingly, miR144a* and miR144b* also appear to target genes required for chromatin remodeling/modification, i.e. *At2g23380*/*CURLY LEAF* and *At2g28290*/*SPLAYED*.

Confirmed targets of miR398a include two Cu/Zn superoxide dismutase genes (*CSD1* and *CSD2*) and *COX5b.1* (cf. introduction). The prediction algorithms detected *CSD1*, *COX5b.1* and *At1g12520*/*CCS1*, a chaperone that activates CSD, as potential targets of miR398a (Table I). *CSD2* was not found, most likely due to a bulge and GU wobble in the seed region of the *CSD2* miR398a duplex (Brodersen and Voinnet, 2009).

DISCUSSION

QRT-PCR of pri-miRs is suitable for discovery of stimulus-dependent miRs.

The role of miRs during the adaptation of plants to abiotic and nutritional stresses is a field that attracts increasing interest (Chiou, 2007; Sunkar *et al.*, 2007), but information on stress dependent expression of *MIRNA* genes is limited. To overcome this situation we developed a qRT-PCR platform for quantification of almost all known Arabidopsis pri-miRs. The results obtained with the platform and from targeted assays for mature miRs show that the responses of pri-miRs frequently match the responses of the biologically active mature species, thus validating pri-miR profiling as a useful discovery tool. It is also rapid, sensitive and inexpensive, and should represent an attractive initial approach for the investigation of *MIRNA* gene expression. The usefulness of the pri-miR platform is also demonstrated by comparative analysis of the *hyl1* mutant and wild-type plants, revealing accumulation of specific pri-miRs in *hyl1* and thus an important role for the HYL1 dsRNA-binding protein in selective pri-miR maturation (Szarzynska *et al.*, 2009). We found only a few examples where the P- or N-response of pri-miRs was not confirmed for the corresponding mature miRs. Although this could have been due to technical reasons, regulation or attenuation at the level of miR maturation could also account for these differences.

It is likely that the number of recognized Arabidopsis *MIRNA* loci will further increase (Lindow and Krogh, 2005, Lindow *et al.*, 2007) especially with deeper analysis of SRS data, possibly reaching numbers similar to those currently known for rice (269), zebra fish (337), mouse (472) and man (678) (cf. http://microrna.sanger.ac.uk). The easily scalable qRT-PCR approach allows regular updates of the platform as new *MIRNA* genes are discovered. In this regard, we invite readers to send us relevant sequence information.

Evidence for miR144 being a true miR.

The novel Pi-responsive miR144 was revealed by a version of miRDeep optimized for analysis of plant sequences (P. May, unpublished), but this alone is not conclusive proof that it is a true miR. A number of revised criteria exist for annotation of plant miRs (Meyers *et al.*, 2008). The primary and only criterion that is necessary and sufficient for annotation as a miR, is conclusive evidence of precise biogenesis from a qualifying stem-loop, and this criterion is met by miR144. First, miR144 was shown to be derived from longer polyA-tailed precursor transcripts, as it was possible to obtain precursor PCR amplicons from cDNA pools generated by reverse transcription with an oligo-dT primer (Figure 4C). Secondly, the two miR144 precursors fold into characteristic hairpin structures with stabilities typical for known miR

precursors. Thirdly, there is precise excision of 21-nucleotide miR144/miR144* duplexes from the two stem-loop precursors (cf. Supplemental File 3). Fourthly, miR144 and miR144a/b* are derived from opposite stem-arms and form duplexes with typical 3´-overhangs of 2-nt length. Fifthly, base pairing between miR144 and the star strands is extensive (Figure 4B), and finally, the observed small RNA abundance corresponds entirely to the duplexes. Ancillary criteria for plant miR annotation include: (i) the existence of target genes, (ii) conservation between species and (iii) biogenesis that is dependent on dicer-like (DCL) proteins. There are obvious potential target genes for miR144 (Table I) although the biological significance of these being targeted by miR144 is as yet unknown. We also detected pre-miR144 homologs and found mature miR144 in rapeseed (Figure 5, Supplemental Figure 9). Although the dependence of miR144 biogenesis on e.g. *DCL1* or *DCL4* still needs to be tested, there is already overwhelming evidence that miR144 is a true miR.

More widespread regulation by small RNAs during P-limitation.

So far, miR399s were the only small RNA species known to strongly increase during P-limitation (see introduction). Five *MIRNA399* genes that encode the slightly different mature miR399s exist in Arabidopsis. Still the only confirmed target of miR399s is *PHO*2, while *IPS1* is a miR399 interactor (Franco-Zorilla *et al.*, 2007). This situation and expansion of the *MIRNA399* gene family in other plant species such as *Medicago truncatula* (F. Krajinski, MPI-MPP, personal communication) and rice (Lindow *et al.*, 2007), however, indicate a larger miR399 regulatory network. The new finding that at least four additional miRs and several miR*s with strong P-status dependent expression exist now suggests that regulation/signaling by small RNAs during P-limitation is even more widespread. Regulatory activity of miR* species and their presence in argonaute complexes has been demonstrated previously in Drosophila (Okamura *et al.*, 2008), but is so far unreported in plants. The fact that the SRS read numbers for some miR* sequences clearly exceed the numbers for the corresponding miRs indicates that they are not merely byproducts that are slowly degraded.

Target predictions and biological processes potentially affected by P-regulated small RNAs.

We used several prediction algorithms and mined degradome data (Table I) to determine likely targets of P-regulated small RNAs. This combinatorial approach revealed several miR targets that were predicted by two or more complementary algorithms, giving greater

confidence in the predictions. Target analysis with PITA also indicated that inclusion of thermodynamics of RNA-RNA interactions can change the results greatly (Hofacker, 2007). Only PITA correctly identified *IPS1*, a non-coding RNA that qualifies as a *bona fide* miR399 target-like interactor (Franco-Zorilla *et al.*, 2007), emphasizing the complementarity and predictive power of PITA. The number of potential targets identified with PITA (Supplemental File 4) further suggests that an individual plant miR could also have a larger range of action, for example, by inducing widespread changes in protein synthesis, as recently reported for several human miRs (Selbach *et al.*, 2008).

Three P-starvation inducible miRs (miR399, miR144, miR827) have confirmed or likely target genes involved in protein degradation via the 26S proteasome. MiR827 targets the E3 ligase gene *NLA* (*At1g02860*). *NLA* transcript also drops 2 to 3-fold during P-limitation when miR827 is highly expressed (Morcuende *et al.*, 2007). NLA is crucial for anthocyanin synthesis and the *nla* mutant displays severely reduced anthocyanin content and early leaf senescence during N-limitation (Peng *et al.*, 2007a, 2007b; 2008). However, during P-limitation or during simultaneous P- and N-limitation the mutant displays wild-type-like anthocyanin levels and no leaf senescence (Peng *et al.*, 2008), showing that the signal derived from P-limitation is sufficient to induce anthocyanin production in the *nla* mutant. The link between P-limitation and *NLA* provided by miR827 (Figure 6A) suggests that NLA activity is actively down-regulated during P-limitation. This could indicate that plants select one or the other input signal depending on nutrient conditions, and therefore the existence of hierarchies in the interplay of macronutrient regulatory networks. MiR144 is predicted to target the E3 ligase gene *At3g27150* (Table I). *At3g27150* displays strictly root-specific expression in large-scale transcriptome datasets like AtGenExpress (Schmid *et al.*, 2005), suggesting it functions in the root. This is interesting in the context of the high abundance of miR144 in phloem sap during Pi-limitation (Figure 5) suggesting another systemic regulatory circuitry, analogous to the miR399 - *PHO2* paradigm (Pant *et al.*, 2008).

Regulation of chromatin status appears to be another biological process influenced by P-limitation-induced miRs, as suggested by the best predicted target genes of miR778, miR144a* and miR144b*, namely: *SUVH6* (*At2g22740*) encoding a SET-domain containing histone methyltransferase, *At2g23380*/*CURLY LEAF* a SET-domain gene required for histone methylation and genetic imprinting (Schubert *et al.*, 2006), and *At2g28290*/*SPLAYED* encoding a chromatin remodeling complex subunit required for maintenance and identity of the shoot apical meristem (Kwon *et al.*, 2005).

MiR398a is strongly reduced in P-, N- and C-limitation (Figure 3) indicating a more general response to nutrient-stress. Repression of miR398a by C-limitation also correlates with its induction by sucrose (Dugas and Bartel, 2008). Targets of miR398a include *CSD1* and *CSD2* (see introduction). CSD is required for detoxification of reactive oxygen species (ROS) that increase during nutrient limitations and other environmental stresses (e.g. heat or drought) (Apel and Hirt, 2004; Shin *et al.*, 2005, Sunkar *et al.*, 2006). Therefore, down-regulation of miR398a leading to higher CSD activity would be an appropriate response to nutrient stress.

Potential biological impact of miR169 regulation by N availability.

The targets of miR169s are several HAP2 transcription factors i.e. nuclear factor YA subunits (NF-YA) (Table I; Combier *et al.*, 2006; Fahlgren *et al.*, 2007; Li *et al.*, 2008). Transcripts of several of these genes, including *At3g05690*/*NF-YA2*, *At1g54160*/*NF-YA5*, *At3g14020*/*NF-YA6*, *At1g72830*/*NF-YA8* and *At5g06510*/*NF-YA10*, increase during N- and P-limitation (Supplemental Figure 10; Scheible *et al.*, 2004; qRT-PCR confirmation not shown), thereby showing the opposite response compared to miR169.

In Arabidopsis, miR169 was reported to influence drought resistance via inhibition of the A5 subunit of NF-Y, a ubiquitous transcription factor that is highly expressed in guard cells and crucial for the expression of a number of drought stress-responsive genes (Li *et al.*, 2008). *Nfya5* knockout mutants and plants over-expressing miR169 show enhanced leaf water loss and are more sensitive to drought stress, whereas *NFYA5* over-expressers show the opposite phenotypes (Li *et al.*, 2008). In addition to the effects of the nitrate-transporter CHL1 (Guo *et al.*, 2003) or nitrate reductase-mediated nitric oxide generation (Desikan *et al.*, 2002) on stomatal opening, low expression of miR169 during N-limitation could thus contribute to drought-tolerance of N-limited plants (Lodeiro *et al.*, 2000; Castaings *et al.*, 2008).

In legume species, nodule development is dependent on the presence of previously established nodules and N/nitrate availability, creating a root-to-shoot signal that activates the CLAVATA1-like receptor kinase SUNN in *Medicago truncatula* or HAR1 in *Lotus japonicus*. A recent report suggests that a nitrate-induced CLAVATA3/ESR-related (CLE) peptide is this root-to-shoot signal (Figure 6B, Okamoto *et al.*, 2009). HAR1 exerts negative shoot control of root nodulation (Krusell *et al.*, 2002; Nishimura *et al.*, 2002) through a shoot-to-root signal that might include auxin transport (van Noorden *et al.*, 2006). It is also known that the miR169 target gene *HAP2-1* in *Medicago truncatula* is a key regulator for

differentiation of nodule primordia (Combier *et al.*, 2006) (Figure 6B). MiR169 over-expression or knockdown of *HAP2-1* leads to a developmental block of nodule formation (Combier *et al.*, 2006). Repression of miR169s by N-limitation, as detected in our experiments, points towards a potential mechanistic link between low N-status and nodule-development in legumes. High abundance of miR169 in phloem sap during N-replete growth and the sharp decrease during N- and P-limitation (Figure 5) also flags miR169 as a potential long-distance signal (Figure 6B) that is able to report shoot N- and P-status to the roots, similar to the role of miR399 (Pant *et al.*, 2008). It will be interesting to test whether miR169 abundance is increased by nitrate/N in legumes and whether miR169 expression and/or phloem abundance is dependent on *SUNN*/*HAR1*, to establish if this is a novel shoot-to-root signal for control of nodule differentiation.

CONCLUSION

MiRs are emerging as increasingly interesting (systemic) regulators during mineral nutrient stress in plants. The discovery of new nutrient-dependent miRs opens up the possibility of testing their roles and those of their predicted targets during adaptation of plants to nutrient deficiency. The qRT-PCR platform described in this paper serves as a useful initial approach to test the response of annotated miRs in a given biological scenario, providing opportunities to discover new signaling and regulatory networks.

MATERIALS AND METHODS

Plant materials.

Nine-day-old nutrient-replete, nitrogen (N) -, phosphorus (P) - or carbon (C) -limited wild-type *Arabidopsis thaliana* Col-0 seedlings were grown in sterile liquid cultures as previously described (Scheible *et al.*, 2004, Morcuende *et al.*, 2007; Osuna *et al.*, 2007). The physiological status of the plant materials was confirmed by expression analysis of marker genes (cf. Supplemental Figure 5) prior to qRT-PCR analysis. Rapeseed (*Brassica napus* cv. Drakkar) was germinated and grown hydroponically (cf. Buhtz *et al.*, 2008) in a full nutrient solution (FNS) containing 4 mM N and 0.5 mM P. After 47 days, plants were divided into three sets and one set was supplied with lower N (2mM KNO3) NS, one with low P (0.1M KPi) NS and one with FNS. From day 61 onwards, i.e. approximately one week before flowering started, low N, low P and FN plants were supplied with nutrient solutions

containing no N, no P or FNS, respectively. N- or P-limited plants developed clear signs of N- or P-starvation (e.g. reduced leaf biomass, earlier flowering, reduced chlorophyll in –N leaves; not shown). Phloem sap was sampled between days 72 and 82 as previously described and is not significantly contaminated by cell sap from other tissues (Giavalisco *et al*., 2006, Buhtz *et al*., 2008).

Primer design and qRT-PCR analysis.

A first set of pri-miR primers (pri-miR156 through 404) was designed by Eurogentec (Liège, Belgium). Primers for pri-miR405 through 870, and primers that replaced malfunctioning primers from the first set, were designed using Primer Express 2.0.0 (Applied Biosystems) and Oligo 6.71 (Molecular Biology Insights, West Cascade, CO). To ensure maximum specificity and efficiency during PCR amplification of pri-miR cDNA under a standard set of reaction conditions (cf. Figure 1A), a stringent set of criteria was used for primer design. This included predicted melting temperatures (Tm) of 61±2°C, limited self-complementarity and PCR amplicon lengths of 50 to 150 base pairs (bp). Secondary hits were minimized by aligning primer candidates to all known Arabidopsis transcript sequences via BLAST searches and eliminating primer pairs with more than the specific hit. Stem loop sequences for which no satisfactory primers could be found were elongated by 100 bp of flanking genomic sequence on each side before primer design was re-initiated. Annealing sites of the primers on the pri-miR sequence are highlighted in Supplemental File 1. Sequences of the qRT-PCR primers are given in Supplemental File 2. Cartridge-purified primers were purchased from Eurogentec (Liège, Belgium), mixed with the corresponding forward or reverse primer upon arrival to a final concentration of 50 µM each, arrayed in 96 deep-well plates and frozen at -80°C for long-term storage. Working stocks (0.5 µM) of each primer pair were prepared from the storage stocks in two serial 10-fold dilution steps and kept at -20°C for short-term storage and used within two weeks.

RNA isolation, cDNA synthesis and qRT-PCR analysis were carried out as previously described in Czechowski *et al.* (2004); Czechowski *et al.* (2005) and Udvardi *et al.* (2008). Mature miR expression was analysed using the method of Chen *et al.* (2005), as described (Pant *et al.*, 2008). MiR-specific RT stem-loop primers are given in Supplemental Table 1. Primer sequences for marker genes are given in the legend to Supplemental Figure 5.

Isolation of small RNAs, library-preparation and deep sequencing.

Total RNA was isolated with Trizol reagent (Invitrogen), supplemented with 0.5% (w/v) N-lauroylsarcosine sodium salt, 3 mM β-mercaptoethanol and 5 mM EDTA. After phase separation, one phenol/chloroform and two chloroform extractions were performed. The aqueous phase (500µl) was mixed with 3 µl glycogen (Roche, 20mg/ml), before RNA was precipitated with 625 µl ethanol and 250 µl 0.8M sodium citrate/1.2M sodium chloride. Samples were incubated for 30 min at R.T. and then centrifuged (25 min, 16.000 g, 4°C). The precipitate was washed with 80% (v/v) ethanol, air-dried and dissolved in 2 mM Tris-HCl (pH 7.5). Efficiency of small RNA extraction and total RNA quality was checked by Northern hybridization with a ^{32}P-labelled oligonucleotide complementary to miR399 (cf. Bari *et al*., 2006). RNA concentration was measured with a NanoDrop ND-1000 (NanoDrop Technologies) and integrity with an Agilent-2100 Bioanalyzer (Agilent Technologies, RNA 6000 NanoChips).

Total RNA from three independent biological replicates (3x20 µg) was mixed with 2x loading buffer II (Ambion), denatured for 2 min at 90°C and separated in a 15% polyacrylamide/7M urea/1xTBE gel, at 300V. Synthetic, phosphorylated 18-mer and 24-mer RNA markers (Biomers.net) and a 10bp DNA ladder (Invitrogen) were used to localize small RNAs (18-30 nt), as well as ligation- and PCR-products, in gels stained with SYBR Gold (Invitrogen). RNA and PCR products were eluted from polyacrylamide gels in 300 µl of EBR buffer (50 mM Mg-acetate, 0.5 M ammonium acetate, 1 mM EDTA, 0.1% SDS) (Reyes and Abelson, 1989) for 10-16h at 20-25°C (300rpm). After phenol/chloroform and chloroform extraction, the aqueous phase was mixed with 1 µl of glycogen and 900 µl of 96% (v/v) ethanol, then cooled to -20°C for 2h and centrifuged (25 min, 16.000 g, 4°C). The RNA pellet was washed twice with 75% (v/v) ethanol and dissolved in 6 µl water.

5´- and 3´-RNA adaptor ligations with RNA primers, reverse transcription and PCR were performed according to Lu *et al*. (2007), except for a 3´-RNA adaptor 3´-end modification consisting of a C3 hydrocarbon spacer (Biomers.net). The PCR reaction (25 µl) was terminated with 75 µl stop buffer (10 mM Tris-HCl pH=8.0, 1 mM EDTA, 0.4 M ammonium acetate). After phenol (pH=8.0) / chloroform extraction, 1 µl glycogen (Roche, 20mg/ml) and 300 µl ethanol were added to precipitate cDNA. The cDNA was denatured in loading buffer II (Ambion) and separated in a 8% polyacrylamide/7M urea gel. The cDNA band was eluted and precipitated as above. The pellet was washed with 70% (v/v) ethanol, air-dried and dissolved in 14µl water. The cDNA concentration was measured using a NanoDrop ND-1000 and checked by 15% polyacrylamide/7M urea gel electrophoresis with oligonucleotides of known concentration. Quality control was performed by TOPO cloning

and Sanger sequencing of several plasmid clones (Lu *et al.*, 2007). Illumina/Solexa sequencing was performed at GATC Biotech (Konstanz, Germany) for Arabidopsis, and FASTERIS (Geneva, Switzerland) for rapeseed libraries.

Analysis of deep sequencing results.

Sequencing reads of lengths between 15 to 32 nucleotides were used after trimming sequence adapters, low complexity regions, e.g. poly(A), and after removing reads of low quality (containing N-runs, N>12). The read sets from the different conditions were subsequently mapped onto the Arabidopsis genome (TAIR8 assembly) using RazerS software. RazerS is an efficient and generic read mapping tool allowing the user to align reads of arbitrary length using either the Hamming distance or the edit distance. RazerS is part of the generic sequence analysis library Seqan (Doring *et al.*, 2008). Only perfect matches to the genome (i.e. full-length alignments with 100% identity) were retained. To investigate the read distributions for available TAIR8 annotations of genes and transposable elements (available from ftp://ftp.arabidopsis.org/home/tair/Genes/TAIR8_genome_release) and to find statistically significant changes in read distributions we used the chi-square test together with Benjamini-Hochberg p-value correction. The chi-square test is known to have a good predictive power and robustness for gene expression analysis (Man *et al.*, 2000). Normalization of small RNA data was performed by dividing the read number of each individual small RNA sequence by the number of redundant reads (15-32 nt) in each library (cf. Supplemental Tables 2 and 3).

MicroRNA prediction.

Potential microRNAs together with their precursor sequences were predicted using the mirDeep software tool (Friedländer *et al.*, 2008). The mirDeep algorithm was adjusted to plant precursor structures to take account the following features of some plant miRs: (i) longer pre-miRs, (ii) pre-miRs that contain more than one miR sequence, (iii) the more diverse read distribution of sequenced small RNAs on plant pre-miR sequences, and (iv) non-hairpin pre-miR structures (P. May, unpublished).

Target gene predictions.

Candidate miR target genes were determined using publicly available prediction algorithms, including miRU (Zhang, 2005), the target search in WMD2 (Ossowski *et al.*, 2008), the prediction tool in the UEA plant sRNA toolkit (Moxon *et al.*, 2008b) and PITA (Kertesz *et al.*, 2007). The programs were used with their default settings.

Accession Numbers

MiRBase accession numbers for all annotated Arabidopsis miRs are available at http://microrna.sanger.ac.uk/cgi-bin/sequences/mirna_summary.pl?org=ath. GenBank accession numbers for the novel miR144 sequences described in this work are FN391952 (ath-miR144a), FN391950 (ath-miR144b), FN391951 (bna-miR144a) and FN391953 (bna-miR144b).

SUPPLEMENTAL MATERIAL

Supplemental File 1. Arabidopsis miR precursor sequences and primer annealing sites.

Supplemental File 2. Quantitative real-time PCR results for all investigated pri-miR species.

Supplemental File 3. Structures and small RNA reads of P-responsive miRs.

Supplemental File 4. Target gene predictions.

Supplemental Figure 1. Genome arrangement and sequence similarity of miR169i-n precursors.

Supplemental Figure 2. Strong induction of mir395 primary transcripts during sulfur limitation.

Supplemental Figure 3. Melting curves of pri-miR amplicons

Supplemental Figure 4. Sequencing results of four pri-miR amplicons.

Supplemental Figure 5. Marker gene expression in nutrient-limited Arabidopsis seedlings.

Supplemental Figure 6. Strong over-expression of miR399d mimics molecular phenotypes of *pho2* mutants.

Supplemental Figure 7. Number and length distribution of small RNA sequences.

Supplemental Figure 8. Q-RTPCR verification of P-limitation induced small RNA species.

Supplemental Figure 9. MicroRNA144 precursors from rapeseed.

Supplemental Figure 10. Nutrient-dependent expression of HAP2 genes in Arabidopsis.

Supplemental Table 1. Primers used for reverse transcription mature miR and qPCR quantification.

Supplemental Table 2. Read numbers from small RNA sequencing of Arabidopsis libraries.

Supplemental Table 3. Read numbers from small RNA sequencing of rapeseed phloem sap.

ACKNOWLEDGMENTS

We thank Dr. John Lunn (MPI-MPP, Potsdam, Germany) and Dr. Peter Dörner (University of Edinburgh, Edinburgh, UK) for proofreading and suggestions on the manuscript.

LITERATURE CITED

Addo-Quaye C, Eshoo TW, Bartel DP, Axtell MJ (2008) Endogenous siRNA and miRNA targets identified by sequencing of the Arabidopsis degradome. Curr Biol **18:** 758-762

Allen E, Xie Z, Gustafson AM, Carrington JC (2005) microRNA-directed phasing during trans-acting siRNA biogenesis in plants. Cell **121:** 207-221

Apel K, Hirt H (2004) Reactive oxygen species: metabolism, oxidative stress, and signal transduction. Annu Rev Plant Biol **55:** 373-399

Aukerman MJ, Sakai H (2003) Regulation of flowering time and floral organ identity by a MicroRNA and its APETALA2-like target genes. Plant Cell **15:** 2730-2741

Aung K, Lin SI, Wu CC, Huang YT, Su, CL, Chiou TJ (2006) Pho2, a phosphate overaccumulator, is caused by a nonsense mutation in a microRNA399 target gene. Plant Physiol **141:** 1000-1011

Axtell MJ, Bartel DP (2005) Antiquity of microRNAs and their targets in land plants. Plant Cell **17:** 1658-73

Bari R, Pant BD, Stitt M, Scheible WR (2006) PHO2, microRNA399, and PHR1 define a phosphate-signaling pathway in plants. Plant Physiol **141:** 988-999

Bartel DP (2004) MicroRNAs: genomics, biogenesis, mechanism, and function. Cell **116:** 281-297

Bracht J, Hunter S, Eachus R, Weeks P, Pasquinelli AE (2004) Trans-splicing and polyadenylation of let-7 microRNA primary transcripts. RNA **10:** 1586-1594

Brodersen P, Sakvarelidze-Achard L, Bruun-Rasmussen M, Dunoyer P, Yamamoto YY, Sieburth L, Voinnet O (2008) Widespread translational inhibition by plant miRNAs and siRNAs. Science **320**: 1185-1190

Brodersen P, Voinnet O (2009) Revisiting the principles of microRNA target recognition and mode of action. Nat Rev Mol Cell Biol **10:** 141-148

Buhtz A, Springer F, Chappell L, Baulcombe DC, Kehr J (2008) Identification and characterization of smallRNAs from the phloem of Brassica napus. Plant J **53:** 739-749

Cai X, Hagedorn CH, Cullen BR (2004) Human microRNAs are processed from capped, polyadenylated transcripts that can also function as mRNAs. RNA **10:** 1957-1966

Castaings L, Camargo A, Pocholle D, Gaudon V, Texier Y, Boutet-Mercey S, Taconnat L, Renou JP, Daniel-Vedele F, Fernandez E, Meyer C, Krapp A (2008) The nodule inception-like protein 7 modulates nitrate sensing and metabolism in Arabidopsis. Plant J **57:** 426-435

Chen C, Ridzon DA, Broomer AJ, Zhou Z, Lee DH, Nguyen JT, Barbisin M, Xu, NL, Mahuvakar VR, Andersen MR, Lao KQ, Livak KJ, Guegler KJ (2005) Real-time quantification of microRNAs by stem-loop RT-PCR. Nucleic Acids Res **33:** e179

Chiou TJ, Aung K, Lin SI, Wu CC, Chiang SF, Su CL (2006) Regulation of phosphate homeostasis by microRNA in Arabidopsis. Plant Cell **18:** 412-421

Chiou TJ (2007) The role of microRNAs in sensing nutrient stress. Plant Cell Environ **30:** 323-332

Chuck G, Candela H, Hake S (2009) Big impacts by small RNAs in plant development. Curr Opin Plant Biol 12**:** 81-86

Combier JP, Frugier F, de Billy F, Boualem A, El-Yahyaoui F, Moreau S, Vernié T, Ott T, Gamas P, Crespi M, Niebel A (2006) MtHAP2-1 is a key transcriptional regulator of symbiotic nodule development regulated by microRNA169 in Medicago truncatula. Genes Dev **20:** 3084-3088

Czechowski T, Bari RP, Stitt M, Scheible WR Udvardi MK (2004) Real-time RT-PCR profiling of over 1400 Arabidopsis transcription factors: unprecedented sensitivity reveals novel root- and shoot-specific genes. Plant J **38:** 366-379

Czechowski T, Stitt M, Altmann T, Udvardi M K, Scheible WR (2005) Genome-wide identification and testing of superior reference genes for transcript normalization in Arabidopsis. Plant Physiol **139:** 5–17

Desikan R, Griffiths R, Hancock J, Neill S (2002) A new role for an old enzyme: nitrate reductase-mediated nitric oxide generation is required for abscisic acid-induced stomatal closure in Arabidopsis thaliana. Proc Natl Acad Sci USA **99:** 16314-16318

De Smet I, Vassileva V, De Rybel B, Levesque MP, Grunewald W, Van Damme D, van Noorden G, Naudts M, Van Isterdael G, De Clercq R, Wang JY, Meuli N, Vanneste S, Friml J, Hilson P, Jürgens G, Ingram GC, Inzé D, Benfey PN, Beeckman T (2008) Receptor-like kinase ACR4 restricts formative cell divisions in the Arabidopsis root. Science **322:** 594-597

Doring A, Weese D, Rausch T, Reinert K (2008) SeqAn an efficient, generic C++ library for sequence analysis. BMC Bioinformatics **9:** 11

Dugas DV, Bartel B (2004) MicroRNA regulation of gene expression in plants. Curr Opin Plant Biol **7:** 512-520

Dugas DV, Bartel B (2008) Sucrose induction of Arabidopsis miR398 represses two Cu/Zn superoxide dismutases. Plant Mol Biol **67:** 403-417

Emery JF, Floyd SK, Alvarez J, Eshed Y, Hawker NP, Izhaki A, Baum SF, Bowman JL (2003) Radial patterning of Arabidopsis shoots by class III HD-ZIP and KANADI genes. Curr Biol **13:** 1768-1774

Fahlgren N, Howell MD, Kasschau KD, Chapman EJ, Sullivan CM, Cumbie JS, Givan SA, Law TF, Grant SR, Dangl JL, Carrington JC (2007) High-throughput sequencing of Arabidopsis microRNAs: Evidence for frequent birth and death of MIRNA genes. PLoS ONE **2:** e219

Franco-Zorrilla JM, Valli A, Todesco M, Mateos I, Puga MI, Rubio-Somoza I, Leyva A, Weigel D, García JA, Paz-Ares J (2007) Target mimicry provides a new mechanism for regulation of microRNA activity. Nat Genet **39:** 1033-1037

Friedländer MR, Chen W, Adamidi C, Maaskola J, Einspanier R, Knespel S, Rajewsky N (2008) Discovering microRNAs from deep sequencing data using miRDeep. Nat Biotechnol **26:** 407-415

Fujii H, Chiou TJ, Lin SI, Aung K, Zhu JK (2005) A miRNA involved in phosphate-starvation response in Arabidopsis. Curr Biol **15:** 2038-2042

German MA, Pillay M, Jeong DH, Hetawal A, Luo S, Janardhanan P, Kannan V, Rymarquis LA, Nobuta K, German R, De Paoli E, Lu, C, Schroth G, Meyers BC, Green PJ (2008) Global identification of microRNA-target RNA pairs by parallel analysis of RNA ends. Nat Biotechnol **26:** 941-946

Giavalisco P, Kapitza K, Kolasa A, Buhtz A, Kehr J (2006) Towards the proteome of Brassica napus phloem sap. Proteomics **6:** 896-909

Gifford ML, Dean A, Gutierrez RA, Coruzzi GM, Birnbaum KD (2008) Cell-specific nitrogen responses mediate developmental plasticity. Proc Natl Acad Sci USA **105:** 803-808

Guo FQ, Young J, Crawford NM (2003) The nitrate transporter AtNRT1.1 (CHL1) functions in stomatal opening and contributes to drought susceptibility in Arabidopsis. Plant Cell **15:** 107-117

Hofacker IL (2007) How microRNAs choose their targets. Nat Genet **39:** 1191-1192

Jones-Rhoades MW, Bartel DP (2004) Computational identification of plant microRNAs and their targets, including a stress-induced miRNA. Mol Cell **14:** 787–799

Kawashima CG, Yoshimoto N, Maruyama-Nakashita A, Tsuchiya YN, Saito K, Takahashi H, Dalmay T (2008) Sulphur starvation induces the expression of microRNA-395 and one of its target genes but in different cell types. Plant J **57:** 313-321

Kertesz M, Iovino N, Unnerstall U, Gaul U, Segal E (2007) The role of site accessibility in microRNA target recognition. Nat Genet **39:** 1278-1284

Kidner CA, Martienssen RA (2005) The developmental role of microRNA in plants. Curr Opin Plant Biol **8:** 38–44

Krusell L, Madsen LH, Sato S, Aubert G, Genua A, Szczyglowski K, Duc G, Kaneko T, Tabata S, de Bruijn F, Pajuelo E, Sandal N, Stougaard J (2002) Shoot control of root development and nodulation is mediated by a receptor-like kinase. Nature **420:** 422-426

Kurihara Y, Watanabe Y (2004) Arabidopsis micro-RNA biogenesis through Dicer-like 1 protein functions. Proc Natl Acad Sci USA **101:** 12753-12758

Kutter C, Schöb H, Stadler M, Meins F Jr, Si-Ammour A (2007) MicroRNA-mediated regulation of stomatal development in Arabidopsis. Plant Cell **19:** 2417-2429

Kwon CS, Chen C, Wagner D (2005) WUSCHEL is a primary target for transcriptional regulation by SPLAYED in dynamic control of stem cell fate in Arabidopsis. Genes Dev **19:** 992-1003

Lai EC (2004) Predicting and validating microRNA targets. Genome Biol. **5:** 115

Lee Y, Kim M, Han J, Yeom KH, Lee S, Baek SH, Kim VN (2004) MicroRNA genes are transcribed by RNA polymerase II. EMBO J **23:** 4051-4060

Li WX, Oono Y, Zhu J, He, XJ, Wu, JM, Iida K, Lu, XY, Cui X, Jin H, Zhu JK (2008) The Arabidopsis NFYA5 transcription factor is regulated transcriptionally and posttranscriptionally to promote drought resistance. Plant Cell **20:** 2238-2251

Lin SI, Chiang SF, Lin WY, Chen JW, Tseng CY, Wu, PC, Chiou TJ (2008) Regulatory network of microRNA399 and PHO2 by systemic signaling. Plant Physiol **147:** 732-746

Lindow M, Krogh A (2005) Computational evidence for hundreds of non-conserved plant microRNAs. BMC Genomics **13:** 119

Lindow M Jacobsen A, Nygaard S, Mang Y, Krogh A (2007) Intragenomic Matching Reveals a Huge Potential for miRNA-Mediated Regulation in Plants. PLoS Comput Biol **3:** e238

Liu HH, Tian X, Li, YJ, Wu CA, Zheng CC (2008) Microarray-based analysis of stress-regulated microRNAs in Arabidopsis thaliana. RNA **14:** 836-843

Lodeiro AR, González P, Hernández A, Balagué LJ, Favelukes G (2000) Comparison of drought tolerance in nitrogen-fixing and inorganic nitrogen-grown common beans. Plant Sci **154:** 31-41

Lu C, Meyers BC, Green PJ (2007) Construction of small RNA cDNA libraries for deep sequencing. Methods **43:** 110–117

Man MZ, Wang X, Wang Y (2000) POWER_SAGE: comparing statistical tests for SAGE experiments. Bioinformatics **16(11)**, 953-959

Meyers BC, Axtell MJ, Bartel B, Bartel DP, Baulcombe D, Bowman JL, Cao X, Carrington JC, Chen X, Green PJ, Griffiths-Jones S, Jacobsen SE, Mallory AC, Martienssen RA, Poethig RS, Qi, Y, Vaucheret H, Voinnet O, Watanabe Y, Weigel D, Zhu JK (2008) Criteria for Annotation of Plant MicroRNAs. Plant Cell **20:** 3186-3190

Morcuende R, Bari R, Gibon Y, Zheng W, Pant BD, Bläsing O, Usadel B, Czechowski T, Udvardi MK, Stitt M, Scheible WR (2007) Genome-wide reprogramming of metabolism and regulatory networks of Arabidopsis in response to phosphorus. Plant Cell Environ **30:** 85-112

Moxon S, Jing R, Szittya G, Schwach F, Rusholme P, Pilcher RL, Moulton V, Dalmay T (2008a) Deep sequencing of tomato short RNAs identifies microRNAs targeting genes involved in fruit ripening. Genome Res **18:** 1602-1609

Moxon S, Schwach F, Dalmay T, Maclean D, Studholme DJ, Moulton V (2008b) A toolkit for analysing large-scale plant small RNA datasets. Bioinformatics **24:** 2252-2253

Nishimura R, Hayashi M, Wu, GJ, Kouchi H, Imaizumi-Anraku H, Murakami Y, Kawasaki S, Akao S, Ohmori M, Nagasawa M, Harada K, Kawaguchi M (2002) HAR1 mediates systemic regulation of symbiotic organ development. Nature **420:** 426-429

Okamoto S, Ohnishi E, Sato S, Takahashi H, Nakazono M, Tabata S, Kawaguchi M (2009) Nod factor/nitrate-induced CLE genes that drive HAR1-mediated systemic regulation of nodulation. Plant Cell Physiol **50:** 67-77

Okamura K, Phillips MD, Tyler DM, Duan H, Chou YT, Lai EC (2008) The regulatory activity of microRNA* species has substantial influence on microRNA and 3' UTR evolution. Nat Struct Mol Biol **15:** 354-363

Ossowski S, Schwab R, Weigel D (2008) Gene silencing in plants using artificial microRNAs and other small RNAs. Plant J **53:** 674-690

Osuna D, Usadel B, Morcuende R, Gibon Y, Bläsing OE, Höhne M, Günter M, Kamlage B, Trethewey R, Scheible WR, Stitt M (2007) Temporal responses of transcripts, enzyme activities and metabolites after adding sucrose to carbon-deprived Arabidopsis seedlings. Plant J **49:** 463-491

Palatnik JF, Allen E, Wu X, Schommer C, Schwab R, Carrington JC, Weigel D (2003) Control of leaf morphogenesis by microRNAs. Nature **425:** 257-263

Pant BD, Buhtz A, Kehr J, Scheible WR (2008) MicroRNA399 is a long-distance signal for the regulation of plant phosphate homeostasis. Plant J **53:** 731-738

Peng M, Hannam C, Gu H, Bi YM, Rothstein SJ (2007a) A mutation in NLA, which encodes a RING-type ubiquitin ligase, disrupts the adaptability of Arabidopsis to nitrogen limitation. Plant J **50:** 320-337

Peng M, Bi YM, Zhu T, Rothstein SJ (2007b) Genome-wide analysis of Arabidopsis responsive transcriptome to nitrogen limitation and its regulation by the ubiquitin ligase gene NLA. Plant Mol Biol **65:** 775-797

Peng M, Hudson D, Schofield A, Tsao R, Yang R, Gu H, Bi YM, Rothstein SJ (2008) Adaptation of Arabidopsis to nitrogen limitation involves induction of anthocyanin synthesis which is controlled by the NLA gene. J Exp Bot **59:** 2933-2944

Ramakers C, Ruijter JM, Deprez RH, Moorman AF (2003) Assumption-free analysis of quantitative real-time polymerase chain reaction (PCR) data. Neurosci Lett **339:** 62–66

Rhoades MW, Reinhart BJ, Lim LP, Burge CB, Bartel B, Bartel DP (2002) Prediction of plant microRNA targets. Cell **110:** 513-520

Scheible WR, Morcuende R, Czechowski T, Fritz C, Osuna D, Palacios-Rojas N, Schindelasch D, Thimm O, Udvardi M K, Stitt M (2004) Genome-wide reprogramming of primary and secondary metabolism, protein synthesis, cellular growth processes, and the regulatory infrastructure of Arabidopsis in response to nitrogen. Plant Physiol **136:** 2483-2499

Schmid M, Davison TS, Henz SR, Pape UJ, Demar M, Vingron M, Schölkopf B, Weigel D, Lohmann JU (2005) A gene expression map of Arabidopsis thaliana development. Nat Genet **37:** 501-506

Schmittgen TD, Jiang J, Liu Q, Yang L (2004) A high-throughput method to monitor the expression of microRNA precursors. Nucleic Acids Res **32:** e43

Schubert D, Primavesi L, Bishopp A, Roberts G, Doonan J, Jenuwein T, Goodrich J (2006) Silencing by plant Polycomb-group genes requires dispersed trimethylation of histone H3 at lysine 27. EMBO J **25:** 4638-4649

Selbach M, Schwanhäuser B, Thierfelder N, Fang Z, Khanin R, Rajewsky N (2008) Widespread changes in protein synthesis by microRNAs. Nature **455:** 58-63

Sharma VK, Ramirez J, Fletcher JC (2003) The Arabidopsis CLV3-like (CLE) genes are expressed in diverse tissues and encode secreted proteins. Plant Mol Biol **51:** 415-425

Shi R, Chiang VL (2005) Facile means for quantifying microRNA expression by real-time PCR: Biotechniques **39:** 519-525

Shin R, Berg RH, Schachtman DP (2005) Reactive oxygen species and root hairs in Arabidopsis root response to nitrogen, phosphorus and potassium deficiency. Plant Cell Physiol **46:** 1350-1357

Sunkar R, Zhu JK (2004) Novel and stress-regulated microRNAs and other small RNAs from Arabidopsis. Plant Cell **16:** 2001-2019

Sunkar R, Kapoor A, Zhu JK (2006) Posttranscriptional induction of two Cu/Zn superoxide dismutase genes in Arabidopsis is mediated by downregulation of miR398 and important for oxidative stress tolerance. Plant Cell **18:** 2051-2065

Sunkar R, Chinnusamy V, Zhu J, Zhu JK (2007) Small RNAs as big players in plant abiotic stress responses and nutrient deprivation. Trends Plant Sci **12:** 301-309

Szarzynska B, Sobkowiak L, Pant B D, Balazadeh S, Scheible W-R Mueller-Roeber B, Jarmolowski A, Szweykowska-Kulinska Z (2009) Gene structures and processing of Arabidopsis thaliana HYL1-dependent pri-miRNAs. Nucleic Acids Res doi**:**10.1093/nar/gkp189. PMID: 19304749

Szittya G, Moxon S, Santos DM, Jing R, Fevereiro MP, Moulton V, Dalmay T (2008) High-throughput sequencing of Medicago truncatula short RNAs identifies eight new miRNA families. BMC Genomics **9:** 593

Udvardi MK, Czechowski T, Scheible WR (2008) Eleven Golden Rules of Quantitative RT-PCR. Plant Cell **20:** 1736-1737

van Noorden GE, Ross JJ, Reid JB, Rolfe BG, Mathesius U (2006) Defective long-distance auxin transport regulation in the Medicago truncatula super numeric nodules mutant. Plant Physiol **140:** 1494-1506.

Wu G, Poethig RS (2006) Temporal regulation of shoot development in Arabidopsis thaliana by miR156 and its target SPL3. Development **133:** 3539-3547

Yamasaki H, Abdel-Ghany SE, Cohu CM, Kobayashi Y, Shikanai T, Pilon M (2007) Regulation of copper homeostasis by micro-RNA in Arabidopsis. J Biol Chem **282:** 16369-16378

Yoo BC, Kragler F, Varkonyi-Gasic E, Haywood V, Archer-Evans S, Lee YM, Lough TJ, Lucas WJ (2004) A systemic small RNA signaling system in plants. Plant Cell **16:** 1979-2000

Zhang Y (2005) miRU: an automated plant miRNA target prediction server. Nucleic Acids Res **33:** W701-W714

FIGURE LEGENDS

Figure 1. QRT-PCR platform for pri-miR transcript quantification.

(A) Typical real-time RT-PCR amplification plots of 175 miR amplicons showing increase in SYBR® Green fluorescence (ΔRn, log scale) with PCR cycle number. Note the similar slope of most curves as they cross the fluorescence threshold of 0.18 (green line), which reflects similar amplification efficiency. **(B)** Separation of PCR products on 4% (w/v) high-resolution agarose gels reveals single products of the expected size (black numbers). A selection of ten amplicons is shown. Size standards in bp are indicated to the left. **(C)** Distribution of efficiencies for 154 primer pairs (gray bars). For 21 primer pairs (open bar) no primer efficiencies were obtained in the conditions investigated. **(D)** Expression strength distribution of MIRNA genes (white bars) and of transcription factor genes (black bars). Genes were grouped according to their ΔC_T values, calculated with UBQ10 as reference.

Figure 2. Identification of N-/P-limitation responsive pri-miRs in Arabidopsis.

For each pri-miR species the average $\Delta\Delta C_T$ value ± standard error from three biological replicates (with two technical replicates for each) is depicted. $\Delta\Delta C_T = \Delta C_{T\ FN} - \Delta C_{T\ -nutrient}$, and $\Delta C_T = C_{T\ pri\text{-}miR} - C_{T\ UBQ10}$. Pri-miRs induced in nutrient-limitation thus have a positive $\Delta\Delta C_T$ value and vice versa. The fold induction can be inferred from the equation $(1+E)^{\Delta\Delta C_T}$ where E is PCR efficiency (cf. Supplemental File 2). Only pri-miRs with average $\Delta\Delta C_T$ value >3 or <-3 (as indicated by the light gray shading) are shown. Results for P- and N-limitation are shown as dark gray and open bars, respectively.

Figure 3. Nutrient-responsiveness of mature miRs.

QRT-PCR results are shown for nutrient-replete (white bar), P-limited (black bar), N-limited (gray bar) and carbohydrate-limited (hatched bar) Arabidopsis seedlings. Expression levels are given on a logarithmic scale expressed as $40 - \Delta C_T$, where ΔC_T is the difference in qRT-PCR threshold cycle number of the respective miR and the reference gene *UBQ10* (*At4g05320*); 40 therefore equals the expression level of *UBQ10*; the number 40 was chosen because the PCR run stops after 40 cycles. The results are the average ± standard error of three biological replicates. Significance of the changes found during P-, N- or carbohydrate-limitation was checked with Student's t-test. T-test p-values <0.05 are indicated by a circle, and p-values <0.01 are marked with a plus sign.

Figure 4. P-responsive miRs as detected by small RNA sequencing.

(A) The number of normalized sequence reads (ppm) is shown for all miRs and their corresponding star (*)-strands that show at least a 5-fold change between P-limitation (black bars) and P-replete (open bars) conditions, and for which at least 10 total reads were scored in at least one condition (cf. Supplemental File 3). Normalized read numbers are also shown for a time point of 3 hours after re-supply of 3mM potassium phosphate to previously P-limited seedlings (3h Pi, gray bars). Missing bars indicate zero reads. **(B)** Putative miR144a and b precursor sequences and structures. The sequences of mature miR144 and the presumable star strands are shown in bold on the top and bottom strand, respectively. The number of absolute reads for the three conditions tested (cf. (A)) is indicated. **(C)** QRT-PCR expression of the 82 and 103 nucleotides long pri-miR144a and b amplicons in various conditions (FN, full nutrients; -P, P-limitation; 3hP, 3 hrs Pi re-addition; -N, N-limitation; -C, carbohydrate limitation). Expression levels are plotted on a logarithmic scale as described in the legend to Figure 3. The results are the average ± standard error of three biological replicates with two technical replicates for each.

Figure 5. MicroRNAs with P- or N-status dependent abundance in rapeseed phloem sap.

(A) Abundance of miRs known to be present (miR156, miR159, miR167) or absent (miR171) in rapeseed phloem sap. **(B)** MiR and miR* sequences with P- or N-status dependent abundance. Depicted are normalized read numbers as detected by Solexa sequencing in small RNA libraries prepared from phloem sap samples of phosphate-starved (-P; black bars), nutrient-replete (full nutrition, FN; white bars) and nitrogen-starved (-N; gray bars) rapeseed plants. The significance of the changes between –P (or –N) and full nutrient conditions shown in (B) was analyzed with a Chi-square test and Benjamini-Hochberg p-value correction; p-values <0.0003 are marked with a circle. Sequences of the species shown are: 169m, TGAGCCAAAGATGACTTGCCG; 399, TGCCAAAGGAGATTTGCCCGG; 399-like, TGCCAAAGGAGATTTGTCCGG; 399*-like 1, GGGCGAATACTCTTATGGCAGA; 399*-like 2, GGGCAAGATCTCTATTGGCAGA; 144, TAATCTGCATCCTGAGGTTTA; 144-like, TAATCGGCATCCTGAGGTTTA; 144a*, ATCCTCGGGATACAGATTACC, 144b*, GTCCTCGGGATGCGGATTACC; 144*-like 1, ATCCTCGGGATGCGGATTACC; 144*-like 2, ATCCTCGGGATACGGATTACC; 144*-like 3, ATCCTCGGGACACAGATTACC; 144*-like 4, GACCTCAGGATGCGGATTACC, 144*-like 5, TCCTCGGGATACAGATTACC; 156, TGACAGAAGAGAGTGAGCAC, 159, TTTGGATTGAAGGGAGCTCTA; 167, TGAAGCTGCCAGCATGATCTA; 171, TGATTGAGCCGCGCCAATATC.

Figure 6. Hypothetical models for miR827 and miR169 functions.

(A) Model showing crosstalk between P limitation and N limitation signaling pathways that affect anthocyanin synthesis. **(B)** Model integrating published features of the systemic regulation of nodulation by CLE (Okamoto *et al.*, 2009), SUNN/HAR1 (Krusell *et al.*, 2002), HAP2 and miR169 (Combier *et al.*, 2006), with novel results concerning miR169 described in this work.

TABLES

Table I. Selected targets of P- and N-responsive miRs/miR*s.

miR / miR*	Stimulus	Predicted target gene(s)	Gene product(s)
144	-P	At3g27150[abce]	F-box protein
		At2g23370[abcde]	unknown protein
		At1g07010[abcde]	calcineurin-like phosphoesterase
169a	+N (?)	several *NF-YA*[abcdef]	several nuclear factor Y A subunits
169b/c	+N (?)	several *NF-YA*[abcdef]	several nuclear factor Y A subunits
		At5g42120[abce]	lectin protein kinase family protein
169d-g	+N (?)	several *NF-YA*[abcdef]	several nuclear factor Y A subunits
		At1g70700[ae] At1g48500[be]	jasmonate-ZIM-domain proteins 4 and 9
169h-n	+N, +P	several *NF-YA*[abcdef]	several nuclear factor Y A subunits
		At5g42120[ab]	lectin protein kinase family protein
398a	+P, +N,	At1g08830[bdef]	Cu/Zn superoxide dismutase CSD1
	+C	At1g12520[be]	superoxide dismutase chaperone CCS1
		At3g15640[cd]	cytochrome c oxidase subunit COX5b.1
399a	-P	At2g33770[abcdef]	E2 conjugase PHO2
		At4g09730[ac]	ATP-dependent RNA helicase
		At4g27850[e]	proline-rich protein
399b/c	-P	At2g33770[abcdef]	E2 conjugase PHO2
		At3g59420[abce]	ACR4 kinase
		At3g54700[abc]	phosphate transporter
		At4g00170[bce]	VAMP family protein
		At4g27850[e]	proline-rich protein
		At3g09922[e]	*IPS1*
399d	-P	At2g33770[abcdef]	E2 conjugase PHO2
		At4g09730[ac]	ATP-dependent RNA helicase
399f	-P	At2g33770[abcdef]	E2 conjugase PHO2
		At3g09922[e]	*IPS1*
778	-P	At2g22740[abcde]	histone methyltransferase SUVH6
		At2g35160[a]	histone methyltransferase SUVH5
		At5g51980[e]	WD40-repeat protein
827	-P	At1g02860[abcde]	SPX E3 ligase NLA
		At1g63010[abce]	SPX E3 ligase
144a*	-P	At2g23380[abce]	SET domain protein CURLY LEAF
		At1g60380[abe]	NAC domain transcription factor 24
144b*	-P	At2g28290[e]	SWI2/SNF2-like protein SPLAYED
398a*	+P, +N,	At4g00950[ae]	MEE47 (maternal effect embryo arrest
	+C	At5g06120[abce]	47)
			Ran-binding protein
399c*	-P	At5g64470[abe]	DUF231 protein
399d*	-P	At3g11130[ae]	clathrin heavy chain
399f*	-P	At3g25905[abe]	CLAVATA3/ESR-RELATED 27
778*	-P	Ag1g69610[abe]	ribosomal protein

Predicted by [a] miRU, [b] WMD2, [c] UEA toolbox, [d] degradome data or [e] PITA. [f] Experimentally confirmed.

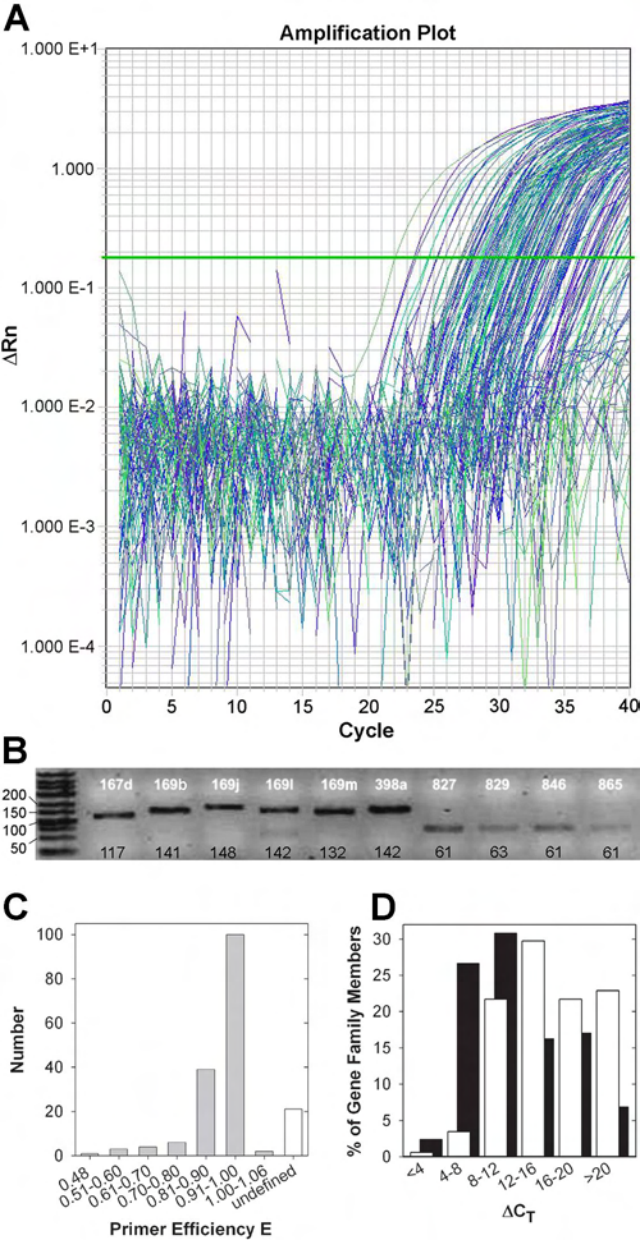
A
Amplification Plot
1.000 E+1
1.000
1.000 E-1
1.000 E-2
1.000 E-3
1.000 E-4
ΔRn
0
5
10
15
20
25
30
35
40
Cycle
B
200
150
100
50
167d
169b
169j
169l
169m
398a
827
829
846
865
117
141
148
142
132
142
61
63
61
61
C
Number
100
80
60
40
20
0
0.48
0.51-0.60
0.61-0.70
0.70-0.80
0.81-0.90
0.91-1.00
1.00-1.06
undefined
Primer Efficiency E
D
% of Gene Family Members
30
25
20
15
10
5
0
<4
4-8
8-12
12-16
16-20
>20
ΔC_T

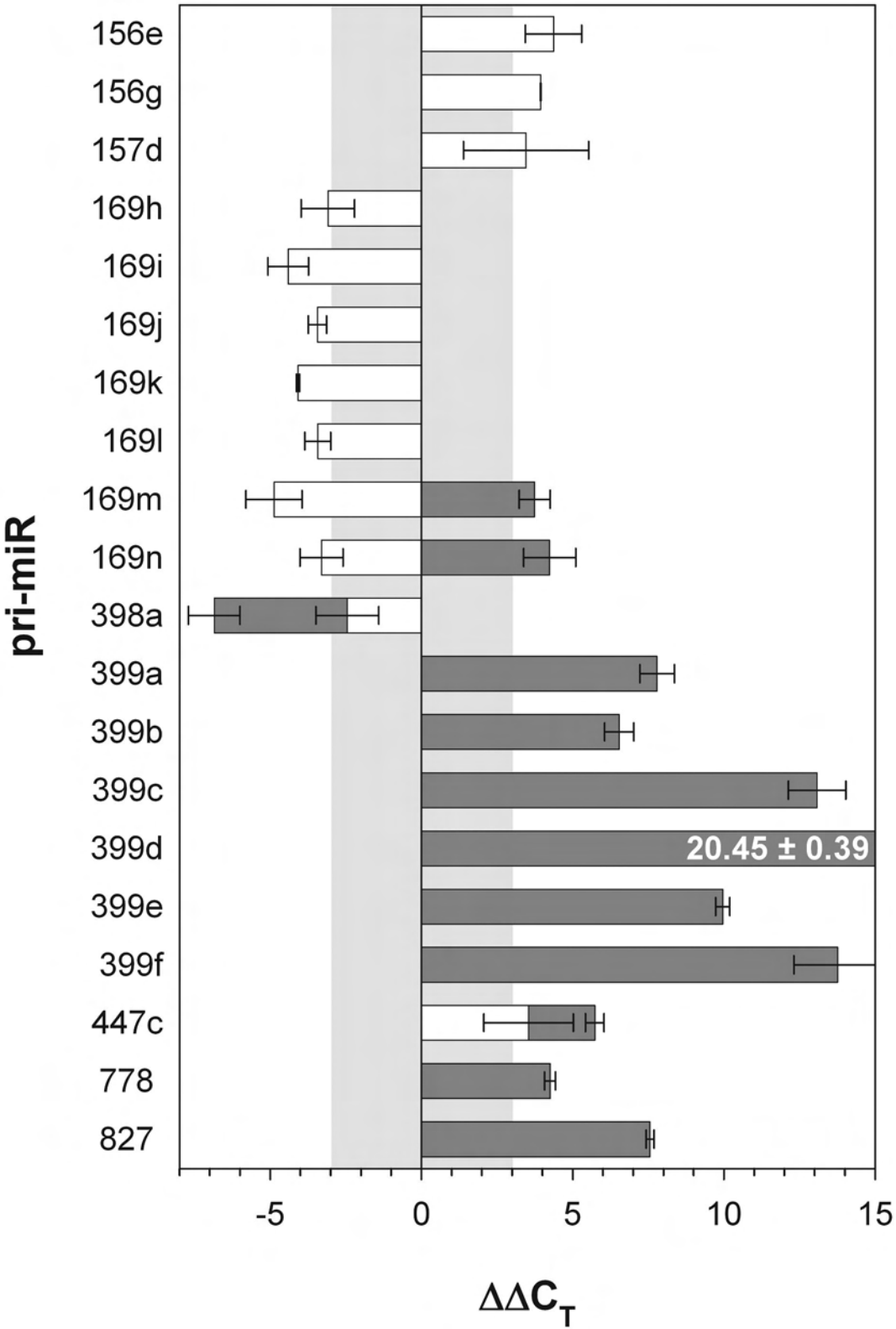
156e
156g
157d
169h
169i
169j
169k
169l
169m
169n
398a
399a
399b
399c
399d
399e
399f
447c
778
827
pri-miR
20.45 ± 0.39
-5
0
5
10
15
ΔΔC_T

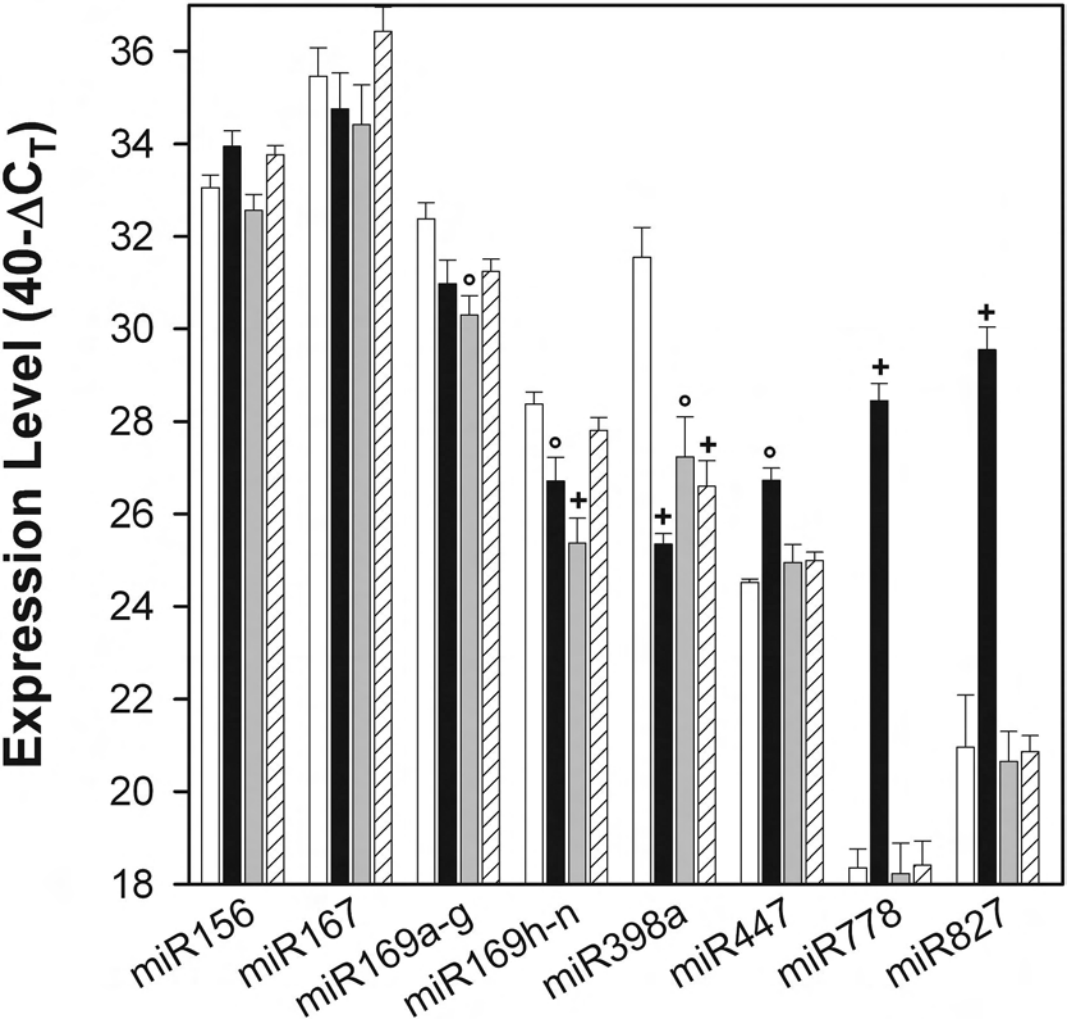
Expression Level (40-ΔC$_T$)
36
34
32
30
28
26
24
22
20
18
miR156
miR167
miR169a-g
miR169h-n
miR398a
miR447
miR778
miR827

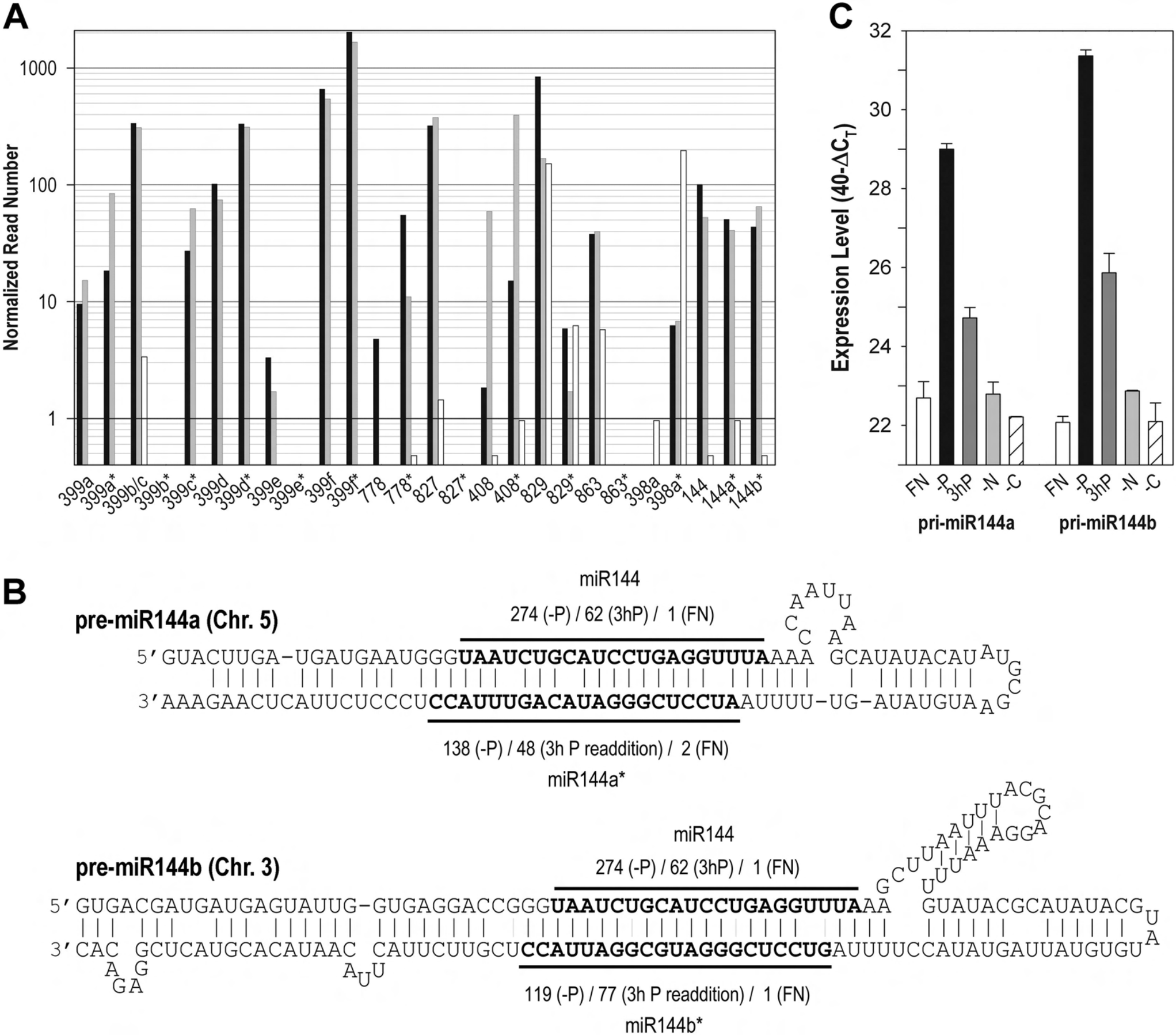
A
Normalized Read Number
1000
100
10
1
399a
399a*
399b/c
399b*
399c*
399d
399d*
399e
399e*
399f
399f*
778
778*
827
827*
408
408*
829
829*
863
863*
398a
398a*
144
144a*
144b*
C
Expression Level (40-ΔC_T)
32
30
28
26
24
22
FN
-P
3hP
-N
-C
pri-miR144a
pri-miR144b
B
pre-miR144a (Chr. 5)
miR144
274 (-P) / 62 (3hP) / 1 (FN)
5′GUACUUGA-UGAUGAAUGGGUAAUCUGCAUCCUGAGGUUUAAAA GCAUAUACAU AUG
3′AAAGAACUCAUUCUCCCUCCAUUUGACAUAGGGCUCCUAAUUUU-UG-AUAUGUA AGC
138 (-P) / 48 (3h P readdition) / 2 (FN)
miR144a*
pre-miR144b (Chr. 3)
miR144
274 (-P) / 62 (3hP) / 1 (FN)
5′GUGACGAUGAUGAGUAUUG-GUGAGGACCGGGUAAUCUGCAUCCUGAGGUUUAAA GUAUACGCAUAUACG U
3′CAC GCUCAUGCACAUAAC CAUUCUUGCUCCAUUAGGCGUAGGGCUCCUGAUUUUCCAUAUGAUUAUGUGU A
119 (-P) / 77 (3h P readdition) / 1 (FN)
miR144b*

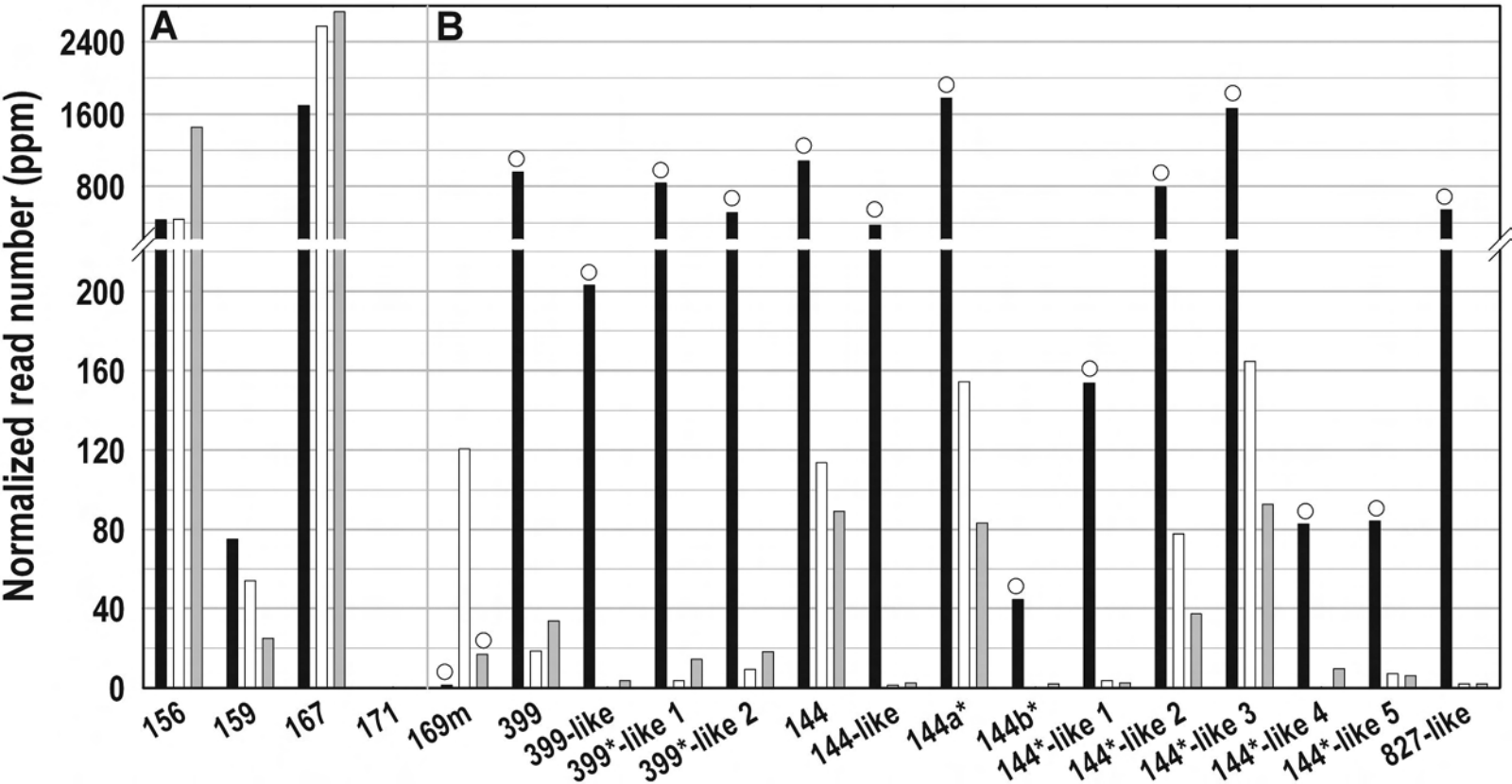
A
B
Normalized read number (ppm)
2400
1600
800
200
160
120
80
40
0
156
159
167
171
169m
399
399-like
399*-like 1
399*-like 2
144
144-like
144a*
144b*
144*-like 1
144*-like 2
144*-like 3
144*-like 4
144*-like 5
827-like

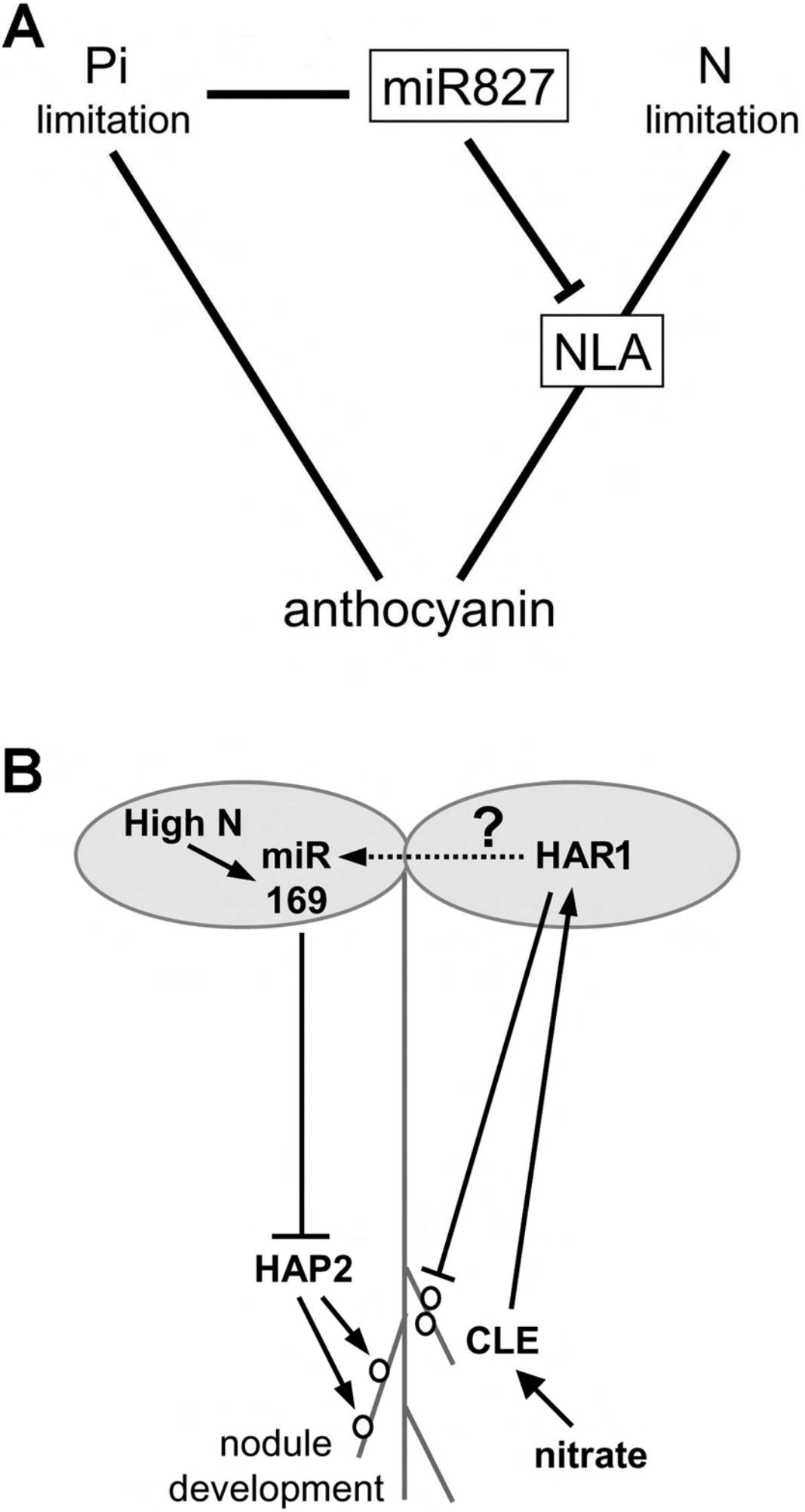
A
Pi
limitation
miR827
N
limitation
NLA
anthocyanin
B
High N
miR
169
?
HAR1
HAP2
CLE
nodule
development
nitrate